Preprint
UCRL-JC-139817

Sound Speeds of Post-Failure Wave Glass

J. U. Cazamias, P. S. Fiske, S. J. Bless

This article was submitted to Hypervelocity Impact Society Symposium, Galveston, Texas, November 6-10, 2000

July 25, 2000

U.S. Department of Energy

Lawrence
Livermore
National
Laboratory

This work was performed under the auspices of the United States Department of Energy by the University of California, Lawrence Livermore National Laboratory under contract No. W-7405-Eng-48.

Sound Speeds of Post-Failure Wave Glass

J.U. Cazamias,[a] P.S. Fiske,[b] S.J. Bless[a]

[a]Institute for Advanced Technology, 4030 W. Braker Lane, Suite 200, Austin, TX 78759

[b]Lawrence Livermore National Laboratory, Box 808, L-45, Livermore, CA 94551

Plate impact experiments were performed on B270 glass in order to measure the properties of post-failure wave material. The initial failure wave velocity is 1.27 km/s. After the material is released, the failure wave velocity drops to 0.65 km/s. At a stress of 6.72 GPa, the sound speed in the failed material is 4.97 km/s (compare to 5.79 km/s in the intact material) with a density comparable to the predicted shock value. At a stress of 0.26 GPa, the average sound speed in the failed material is 3.55 km/s, and the density drops to 65% of the intact value. The spall strength of the failed material is greater than 0.14 GPa.

1. INTRODUCTION

Since failure waves were first observed [1], there has been a considerable amount of effort expended to explain them. See [2] for a general overview and [3] for a more in-depth review of the work performed at Cavendish Laboratory.

There are diverse observations of glass that has experienced a failure wave, and they are not all consistent. Failed glass has a lower impedance than the unfailed material [1]. The longitudinal stress does not significantly change through the failure wave [4]. The failed material has nearly zero spall strength, and its shear strength is significantly degraded [5]. It should be noted that glass densifies, but this behavior is associated with the Hugoniot Elastic Limit (HEL) [6]. The longitudinal strain in front of the failure wave is smaller than predicted elastically, but it increases to the elastic prediction behind the failure wave [7]. The transverse strain remains constant (i.e., 0) behind the failure wave [7]. The sound speed of the failed material does not differ from that of the original specimen [8]. After the first anomalous recompression no further recompressions are observed, suggesting that the impedances have equalized [8]. In [9], pressure-shear experiments were performed. With glass plates impacting steel targets, measurements of the longitudinal free surface velocity in the steel showed negligible change in the impedance of the failed glass when the release wave in the steel reached the interface; yet when steel plates impacted glass targets, the expected recompression signal was observed when looking at the free surface of the glass which implies a change in impedance. There is also the issue of dilatency due to the opening of microcracks, but whether dilatency requires a single release wave or the interaction of several waves to open the microcracks is unclear. However, if one is to understand the explosive nature of fracture in glass, dilatency clearly needs to be understood.

In addition to the obvious inconsistencies, there are some additional ones in the above observations. That the sound speed of the failed material remains unchanged, and that the density increases require a higher impedance rather than a lower. That one sees only one reflection off the failure front implies impedance equalization, but a drop in the impedance due to damage followed by a return to its undamaged value does not seem plausible. That the strain is underpredicted in the unfailed elastic region seems to imply that the glass structure has locked with the failure wave as an unlocking mechanism. In the elastic region this behavior implies an increase of modulus which is not reflected in sound speed measurements and is also contradicted by the dispersive nature of many glass Hugoniots below the HEL. Since the predicted Rankine-Hugoniot density

is achieved only after the failure wave passes, it appears that the region behind the elastic wave is in some metastable/unstable state or that the elastic wave is unsteady. Understanding failure waves might actually lie in understanding this phenomenon and not the failure wave itself.

Ginzberg and Rosenberg [8] impacted manganin gauge-instrumented soda-lime glass. In their experiments, the release wave from the free surface of the glass is reflected from the impactor-target interface as a compressive wave, and by measuring arrival times, one can determine the sound speed in the failed region. We have performed a similar experiment using a VISAR to measure shock wave profiles.

2. EXPERIMENTAL PROCEDURE

Copper flyer plates are made to impact B270 glass disks (from Edmund Scientific) using a He single-stage gun at Lawrence Livermore National Laboratory. The targets and impactors were nominally 25 mm in diameter.

We carried out detailed density, shape, and ultrasonic measurements of the glass samples. Densities were measured using a water-based specific gravity measurement system with a precision of 0.001 g/cm^3. Sample thicknesses were determined using a laser ruler and varied by up to 0.015 mm. Compressional and shear ultrasonic velocities were measured at 30 MHz [10, 11]. See Table 1.

Rear surface velocity measurements were carried out using a fiber optic push-pull VISAR system manufactured by Valyn International with a measured response time of 1.5 ns and a delay of 229.4 m/s/fringe. The surface accelerations were fast enough to cause the loss of a fringe in the VISAR data, which we corrected in the data reduction process. One surface of each sample was roughened and then coated with 5000 angstroms of Al in order to create a diffuse reflecting surface optimal for VISAR measurements.

Impactor velocities were measured using two pairs of piezoelectric signal pins at different distances away from the impact surface. Velocities varied between each pair of pins by no more than 6 m/s.

Table 1
Experimental Parameters

	Shot 722	Shot 723
Impact Velocity (m/s)	275	729
Impactor Thickness (mm)	6.02	6.12
ρ_{target} (gm/cm^3)	2.331	2.328
Target Thickness (mm)	2.17	2.18
c_l (km/s)	5.806	5.792
c_s (km/s)	3.439	3.435
c_0 (km/s)	4.236	4.221

3. EXPERIMENTAL DATA

Figure 1 shows the σ-u diagram for the experiments. Gl represents the glass Hugoniot, Cu the copper Hugoniot and FW the failed material Hugoniot.

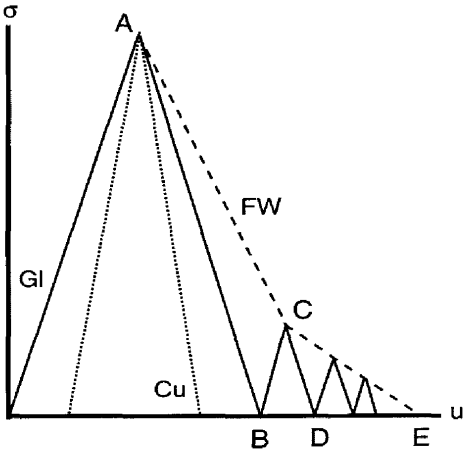

Figure 1. σ-u diagram for Cu-glass impact.

At impact, the glass goes to state A and releases to state B at the rear surface. Ideally, this release wave travels back to the glass-copper interface and, since this interface cannot support tension, the plates separate and no further waves are transmitted. In reality, the release wave is actually a rarefaction fan. The first part reflects off the higher impedance copper as a release wave. After separation occurs, it

reflects as a compression wave which brings the sample back to zero stress. Consequently, the initial release wave is transformed into a thin release-compression wave packet. In the event that a failure wave occurs, when the initial release wave interacts with the failure wave, a small compressive wave propagates into the intact glass, state C, and releases at the free surface to state D. Multiple reflections off of the failure wave may occur. The failure wave eventually reaches the rear surface and releases to state E.

Figure 2 shows the X-t diagram for the experiments. Sound speeds in the material are indicated by ci. Failure wave velocities are indicated by vfi. The positions m, n, w, x, y and z are defined below. The quantities t1, t2 and t3 are the arrival times of the initial compressive wave and its subsequent reflections from the glass surfaces. The time t1 is calculated from the thickness of the plate divided by the wave speed and is taken as the arrival of the wave. The times t2 and t3 are measured from the deepest point of their respective dips. The velocities Δu2 and Δu3 are the depths of the velocity jumps at t2 and t3. The times tf1and tf3 are the arrival times of recompression waves due to the failure wave and are measured from the beginning of their ascent. The velocities Δuf1 and Δuf3 are the velocity jumps at tf1 and tf3. No tf2 is observed (see below).

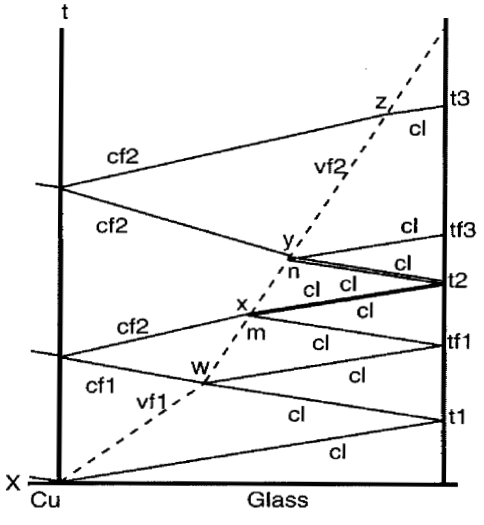

Figure 2. X-t diagram for Cu-glass impact. The double lines near t2 represent nearly coincident waves.

Figure 3 shows the velocity-time history for the 275 m/s impact (shot 722). Table 2 shows the measured quantities. There is some structure to the noise on the plateau of the velocity-time history, but since it is essentially small magnitude elastic waves propagating in a zero stress region, the structure was not analyzed. Figure 4 shows the velocity-time history for the 729 m/s impact (shot 723). Table 2 shows the measured quantities. There is a small velocity increase and decrease after t3, but it is not resolvable. Figure 5 shows an expanded region of Figure 4.

Table 2
Experimental Results

	Shot 722	Shot 723
u_{el} (m/s)	395±5	997±5
Stress (GPa)	2.67	6.72
Width u_{el} (ns)	9±3	67±4
t1 (ns)	374	376
t2 (ns)	1132±2	1240±20
Width t2 (ns)	42±6	180±10
t3 (ns)	1888±2	2350±10
Width t3 (ns)	16±5	260±20
tf1 (ns)	n/a	826±3
tf3 (ns)	n/a	1500±20
Δu2 (m/s)	61±2	14±2
Δu3 (m/s)	59±2	20±4
Δuf1 (m/s)	n/a	38±7
Δuf3 (m/s)	n/a	13±5

4. ANALYSIS

In the following analysis, the measured longitudinal wave speed is used for the sound speed in the unfractured glass. Since the experiments all occur below the HEL, we believe that this is a good approximation.

For material in state A (Figure 1), Lagrangian distances γ will be corrected by $\gamma' = \gamma(\rho_0/\rho) = \gamma(1 - u_{el}/(2c_l))$ (conservation of mass). This might not be correct [7], but it is better

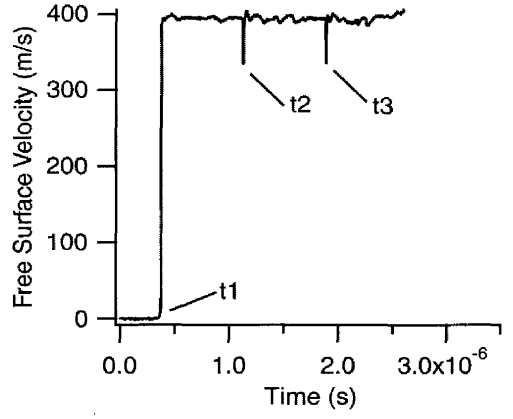

Figure 3. (Shot 722) Velocity-time history for 250 m/s impact.

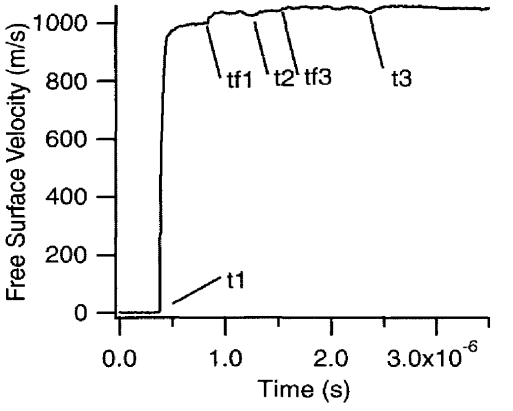

Figure 4. (Shot 723) Velocity-time history for 729 m/s impact.

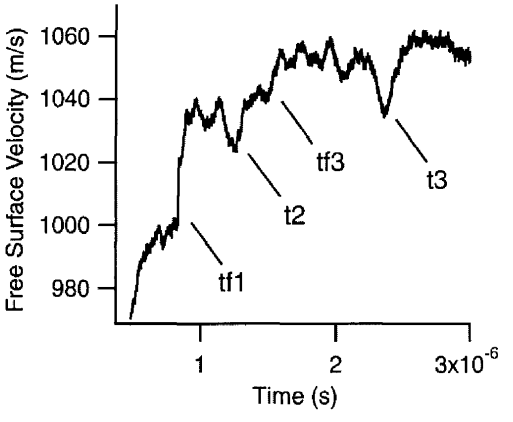

Figure 5. (Shot 723) Expanded region of velocity-time history for 729 m/s impact.

than not correcting the data. Other states' corrections are less than 0.5% and will be ignored.

Taking the plate radius and dividing by the wave speed gives a conservative temporal estimate of when edge effects might matter. For these experiments, it is roughly 2.1 μs. Only t3 in shot 723 occurs after this time. Since its velocity profile correlates well with the signal at t2, we consider it a valid signal.

4.1 Shot 722

Taking distances divided by differential times, the average wave speed is 5.63 km/s for the t1-t2 region, and the average wave speed is 5.74 km/s for the t2-t3 region. While spall does not occur, the pullback signals u2 and u3 allow one to calculate a lower bound for the spall strength $\sigma_{sp} > 0.5\rho c\Delta u$ = 0.4 GPa which is consistent with the expected value of several GPa.

4.2 Shot 723

For tf1, the failure wave is w = 1.36 mm from the rear surface when the release wave reflects off of it at 591 ns:

$$w = \frac{c_l(tf1 - t1)}{1 + \rho_0/\rho}.$$

This implies that the failure wave has traveled at v_{f1} = 1.27 km/s. The state of stress of the material surrounding the failure wave due to the release of the free surface can be estimated by

$$\sigma = \rho_0 c_l \frac{\Delta uf1}{2} = 0.26 \text{ GPa}.$$

Using these numbers, the recompression signal should reflect off the failure wave again when it is 0.87 mm from the rear surface with a corresponding rear surface arrival time of 1126 ns. No such signal is observed. Taking into account: 1) failure waves slow down [4], 2) the released material might not have enough energy to feed the wave, 3) Δu3 > Δu2, 4) small average velocity jump (~5 m/s) from before and after the t2 signal, and 5) the additional structure that t2 possesses as compared to t3 (Figure 5), we postulate that the recompression signal is embedded in the signal centered at t2 (1240 ns). Assuming this,

let m and n be the positions of the failure wave from the rear surface when the second and third reflections, respectively, occur. Then

$$\frac{w-m}{v_{f2}} = \frac{w+m}{c_l}$$

$$\frac{2m+2n}{c_l} = tf3 - tf1$$

$$\frac{m-n}{v_{f2}} = \frac{m+n}{c_l}$$

give a new failure wave velocity $v_{f2} = 0.65$ km/s and a tf2 = 1201 ns which is consistent with our conjecture. We believe that the failure wave velocity drop is due to the low state of stress surrounding the wave.

Disregarding arguments 3 through 5 above, one could postulate that the signal at tf3 is the reflection of the t2 signal, but since t2 and the calculated tf2 are so close, this gives $v_{f2} = 0.78$ km/s which will not qualitatively change our subsequent analysis. There is a problem with this interpretation; namely, the tf3 signal appears too clean to be associated with the actual signal at t2. Given arguments 3 through 5 above and the vagaries associated with pullback signals, we believe that the signal is due to the above postulated tf2 signal.

A third interpretation is to follow [8] and postulate that no further failure wave reflections are observed. This would imply that tf3 represents the failure wave reaching the rear surface with the average failure wave speed increasing to 1.50 km/s. This seems unlikely since the wave velocity has only been observed to move at constant velocity [3] or to slow down [4]. Also, the material on both sides of the failure wave is now near complete release depriving the wave of an energy source for the velocity increase. Finally, the fact that the VISAR signal remains clean after tf3 implies that the surface remains intact, i.e., the failure wave has not reached the rear surface.

A fourth interpretation is to take the break in the velocity jump in the tf1 signal (Figure 5) and associate it with relaxation phenomena in the failed material. This relaxation could result in a double wave structure (elastic-inelastic) in the failed material with the tf3 signal corresponding to the rear surface inelastic wave arrival (Figure 6). In this interpretation tf2 is not inferred, and there are no quantitative measurements of the failure wave velocity other than the tf1 signal which gives $v_f = 1.27$ km/s. A constant failure wave velocity predicts a rear surface arrival time of 1660 ns. Since there is nothing in the record that indicates such an arrival, a change in the failure wave velocity is still implied, but by how much is indeterminate. Without knowledge of the failure wave's location, quantitative measurements of sound speeds are impossible.

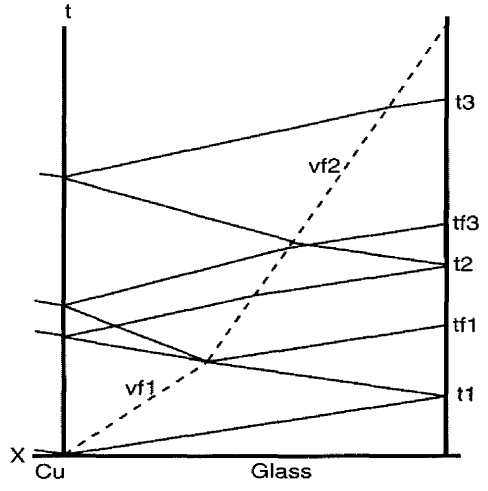

Figure 6. X-t diagram for Cu-glass impact, assuming elastic-inelastic wave structure in failed material.

The time intervals t1-t2 and t2-t3 for shot 723 are significantly larger than for shot 722, implying that the sound speed behind the failure wave is significantly lower than in front of it. This contradicts [8] with two caveats. While failure waves occur with consistent phenomenological properties in a variety of glasses, they did use a different glass (soda lime with $\rho = 2.49$ gm/cm^3, $c_l = 5.84$ km/s, $c_s = 3.46$ km/s). Also, their failed material remained under significant compression while ours did not.

Assuming the existence of the tf2 signal, let w, x, y and z be the distances from the rear surface of the glass where the waves responsible for the t1, t2 and t3 signals intercept the failure wave (see Figure 2). Then with L as the plate thickness, c_{f1} as the wave speed of the compressed failed material (w to Cu interface), and c_{f2} as the wave speed of the released failed material (everywhere else):

$$\frac{w-x}{v_{f2}} = \frac{\frac{\rho_0}{\rho}(L-w)}{c_{f1}} + \frac{(L-x)}{c_{f2}}$$

$$\frac{w-x}{v_{f2}} = (t2-t1) - \frac{\frac{\rho_0}{\rho}w + x}{c_l}$$

$$\frac{x-y}{v_{f2}} = \frac{x+y}{c_l}$$

$$\frac{y-z}{v_{f2}} = \frac{2L-y-z}{c_{f2}}$$

$$\frac{y-z}{v_{f2}} = (t3-t2) - \frac{y+z}{c_l}.$$

These equations give c_{f1} = 4.97 km/s and c_{f2} = 3.55 km/s which imply pressure-dependent properties for the failed material. Since c_{f1} is less than the original sound speed and still under compression, this result contradicts [8].

An estimate for the impedance of the high pressure failed material is

$$Z_f = \rho_f c_{f1} = \frac{\rho_0 c_l (u_{el} - \Delta u_{f1})}{u_{el} + \Delta u_{f1}}$$

which gives Z_f = 12.49 (gm·km)/(cm^3·s). Using c_{f1} = 4.97 km/s, this gives ρ_f = 2.51 gm/cm^3 which compares well to the predicted shock density of 2.54 gm/cm^3 and the results of [7]. Performing a similar calculation for the tf1-tf3 release (taking the base of the tf3 signal at u = 1041 m/s) gives Z_f = 5.35 (gm·km)/(cm^3·s). Using c_{f2} = 3.55 km/s, this gives ρ_f = 1.51 gm/cm^3, implying that dilatency is associated with a single release wave.

A local modulus, $M = \rho c^2$, can now be determined. For the compressed material, M = 62 GPa. This is greater than the original bulk modulus of 41 GPa implying that the failed material still possesses some shear strength. For the released material, M = 19 GPa. This large change in modulus makes estimates of the reference density ambiguous.

One could also calculate the sound speed by assuming it is constant between t1 and t2 and then degrades to another value between t2 and t3 due to damage growth. This gives a t1-t2 sound speed of 4.01 km/s and a corresponding density of 3.10 gm/cm^3 which is clearly inconsistent with [7]. The t2-t3 sound speed is identical to c_{f2}.

While spall does not necessarily occur, the pull-back signal of 20 m/s at t3 allows a calculation of a lower bound for the spall strength $\sigma_{sp} > 0.5\rho_0 c_l \Delta u3$ = 0.14 GPa which seems high for a supposedly comminuted material.

The slight velocity jump after t3 might be due to the arrival of the failure wave.

We have postulated four different interpretations of the data. The issue of whether the tf2 or the t2 signal is the source of the tf3 signal can be tested by striking glass plates of different thicknesses with different impedance impactors so that the arrival times will not overlap and that the shape of t2 will vary. The fourth postulate of a dual wave structure in the failed material can be tested by striking a thick plate of a low impedance material with a thin glass plate which would allow observation of the inelastic wave. The third postulate of a failure wave with increasing velocity, which we consider unlikely, would be viable only in the case of the other postulates being disproven.

5. CONCLUSION

Plate impact experiments were performed on B270 glass in order to measure the properties of post-failure wave material. The initial failure wave velocity is 1.27 km/s. After the material is released, the failure wave velocity drops to 0.65 km/s. At a stress of 6.72 GPa, the sound speed in the failed material is 4.97 km/s (compare to 5.79 km/s in the intact material) with a density comparable to the predicted shock value. At a stress of 0.26 GPa, the average sound speed in the failed material is 3.55 km/s and the density drops to 65% of the intact value. The spall strength of the failed material is greater than 0.14 GPa.

ACKNOWLEDGEMENTS

This work was performed under the auspices of the U.S. Department of Energy by the Lawrence

Livermore National Laboratory under contract number W-7405-ENG-48. J.U. Cazamias and S.J. Bless were supported by the U.S. Army Research Lab under contract DAAA21-93-C-0101. Thanks to A.E. Brown of LLNL who performed the ultrasonic measurements. Thanks to D.W. Baum of LLNL who agreed to support the experiments.

REFERENCES

1. Rasorenov, S.V., Kanel, G.I., Fortov, V.E., Abasehov, M.M., "The Fracture of Glass Under High-Pressure Impulsive Loading," *High Pressure Research,* **6**, 225-232 (1991).
2. Brar, N.S., "Failure Waves in Glass and Ceramics Under Shock Compression," *Shock Compression of Condensed Matter-1999*, 601-606 (2000).
3. Bourne, N., Millett, J., Rosenberg, Z., Murray, N., "On the Shock Induced Failure of Brittle Solids," *J. Mech. Phys. Solids,* **46** (10), 1887-1908 (1998).
4. Kanel, G.I., Rasorenov, S.V., Fortov, V.E., "The Failure Waves and Spallations in Homogenous Brittle Materials," *Shock Compression of Condensed Matter 1991*, 451-454 (1992).
5. Brar, N.S., Bless, S.J., Rosenberg, Z., "Impact-Induced Failure Waves in Glass Bars and Plates," *Appl. Phys. Lett.,* 59 (26), 3396-3398 (1991).
6. Rosenberg, Z., Bourne, N., Millett, J., "Direct Measurement of Strain in Shock-Loaded Glass Specimens," *J. Appl. Phys.*, **79** (8), 3971-3974 (1996).
7. Millett, J., Bourne, N., Rosenberg, Z., "Measurement of Strain in a Shock-Loaded High-Density Glass," *Shock Compression of Condensed Matter-1999*, 607-610 (2000).
8. Ginzberg, A., Rosenberg, Z., "Using Reverberation Techniques to Study the Properties of Shock-Loaded Soda-Lime Glass," *Shock Compression of Condensed Matter-1997*, 529-531 (1998).
9. Clifton, R.J., Mello, M., Brar, N.S., "Effect of Shear on Failure Waves in Soda Lime Glass," *Shock Compression of Condensed Matter-1997*, 521-524 (1998).
10. Papadakus, E.P., "Ultrasonic Diffraction Loss and Phase Change in Anisotropic Materials," *J. Acoust. Soc. Am.,* **40**, 863-876 (1966).
11. Papadakus, E.P., "Ultrasonic Phase Velocity by the Pulse-Echo-Overlap Method Incorporating Diffraction Phase Corrections," *J. Acoust. Soc. Am.,* **42**, 1045-1051 (1967).